Short wavelength fluctuation effects on the magnetization in type I and low-κ type II superconductors

2003 J. Phys.: Condens. Matter 15 3283

(http://iopscience.iop.org/0953-8984/15/19/327)

INSTITUTE OF PHYSICS PUBLISHING JOURNAL OF PHYSICS: CONDENSED MATTER

J. Phys.: Condens. Matter **15** (2003) 3283–3298 PII: S0953-8984(03)56778-9

Short wavelength fluctuation effects on the magnetization in type I and low-κ type II superconductors

J Mosqueira, C Carballeira, S R Currás, M T González, M V Ramallo, M Ruibal, C Torrón and F Vidal[1]

LBTS Unidad Asociada al ICMM, CSIC, Spain
and
Departamento de Física da Materia Condensada, Universidade de Santiago de Compostela, E15782 Santiago de Compostela, Spain

E-mail: fmvidal@usc.es

Received 27 November 2002
Published 6 May 2003
Online at stacks.iop.org/JPhysCM/15/3283

Abstract

The effects on the magnetization of fluctuating Cooper pairs created above the superconducting transition by thermal agitation energy (the so-called fluctuation-induced diamagnetism, FD) have been measured in a clean type I superconductor (Pb) and in a clean low Ginzburg–Landau parameter (κ) type II superconductor (Nb). These experiments extend the earlier measurements of Gollub, Beasley and Tinkham to both the high reduced temperature region ($\varepsilon \equiv \ln(T/T_{C0}) \gtrsim 0.1$) and the high reduced magnetic field region ($h \equiv H/H_{C2}(0) \gtrsim 0.1$). Our data show that in spite of FD being deeply affected in both superconductors by the presence of non-local electrodynamic effects, the superconducting fluctuations sharply vanish when ε or h become of the order of 0.5 and, respectively, 1. This short-wavelength behaviour at high reduced temperatures of the superconducting fluctuations is similar to that previously observed at high reduced temperatures in dirty low-T_C superconductors and in high-T_C cuprates, where the non-local effects are unobservable. These last results suggest that in the short wavelength regime the superconducting fluctuations in clean low-T_C superconductors are still dominated by the uncertainty principle, which imposes a limit to the shrinkage, when ε increases, of the superconducting wavefunction. This may also be the case when $h \to 1$, although the presence of strong non-local effects in these clean and low-κ superconductors may also deeply affect their high field behaviour.

[1] Author to whom any correspondence should be addressed.

0953-8984/03/193283+16$30.00

1. Introduction

At high reduced temperatures, when $\varepsilon \equiv \ln(T/T_{C0}) \gtrsim 0.1$, or at high reduced magnetic fields, when $h \equiv H/H_{C2}(0) \gtrsim 0.1$, thermal fluctuations are deeply affected by the so-called short-wavelength effects, which appear when the characteristic wavelength of the fluctuations becomes of the order of ξ_0, the actual or Pippard superconducting coherence length at $T = 0$ K [1, 2]. In these expressions, T_{C0} is the superconducting transition temperature at zero applied magnetic field (H) and $H_{C2}(0)$ is the upper critical magnetic field amplitude. The behaviour of the superconducting fluctuations in the short wavelength regime is a long standing but still open problem, whose interest has been considerably enhanced by the discovery of high temperature cuprate superconductors (HTSC) [2, 3].

Recent experiments on these fluctuation effects at high reduced temperatures ($\varepsilon \gtrsim 0.1$) on the electrical conductivity (the so-called paraconductivity, $\Delta\sigma$) and on the magnetization (the so-called excess magnetization, ΔM), suggest that the behaviour of the short-wavelength fluctuations is dominated by the uncertainty principle, which imposes a limit on the shrinkage of the superconducting wavefunction when ε increases [3–5]. These measurements were mainly done in HTSC and in dirty low-T_C superconductors, with high or moderate values of the Ginzburg–Landau parameter, $\kappa \equiv \lambda/\xi$, where λ is the magnetic field penetration length and ξ is the superconducting coherence length. Only a few preliminary data were obtained in the high-ε region in low-κ type I or type II superconductors and, in all cases, in the low reduced magnetic field regime, for $h \leqslant 0.2$ [3]. Let us already stress here that as suggested earlier in the pioneering measurements of the fluctuation-induced diamagnetism (FD) of Gollub and co-workers in the low-ε region [1, 2, 6], the superconducting fluctuations in clean low-T_C superconductors may be deeply affected by non-local electrodynamic effects. This is in contrast with the dirty low temperature superconductors (LTSC) and the clean HTSC, with moderate or high κ values, where non-local effects are unobservable [5, 7].

The first aim of this paper is to present detailed FD measurements in a type I superconductor (Pb) and in a low-κ type II superconductor (Nb) in all the ε and h regions above T_{C0}. As noted before, the FD in these clean low-κ superconductors is appreciably affected for all experimentally accessible ε and h by non-local effects [1, 2, 6]. So, the first question we will experimentally address here is whether the FD in the high-ε region will be still dominated, even in the presence of important non-local effects, by the Heisenberg localization energy associated with the shrinkage, at high reduced temperatures, of the superconducting wavefunction. In addition, we will extend these FD experiments to the high reduced field regime. We will see here that these last measurements suggest that the FD effects also vanish (at all temperatures) when $h \approx 1$. Here we will then argue that this striking result may still be understood at a qualitative level in terms of the limitations imposed by the indetermination principle to the shrinkage of the superconducting wavefunction when h increases. However, the non-local effects may also severely suppress the fluctuations when $h \to 1$ in these clean and low-κ superconductors. Although these non-local electrodynamic effects have been studied theoretically by different authors [1, 2, 8, 9], to the best of our knowledge, at present, a unified approach allowing a quantitative analysis of these effects at high reduced temperatures does not exist. So, we will compare our experimental results with the Gaussian–Ginzburg–Landau (GGL) approach under different cutoff conditions [3–5], that takes into account the short wavelength effects on the conventional mean-field-like description without non-local effects.

2. Experimental details

The samples used in these experiments were a commercial Nb single crystal (Goodfellow, 99.99% purity) and a Pb polycrystal (Goodfellow, 99.9999%) in the form of cylinders of

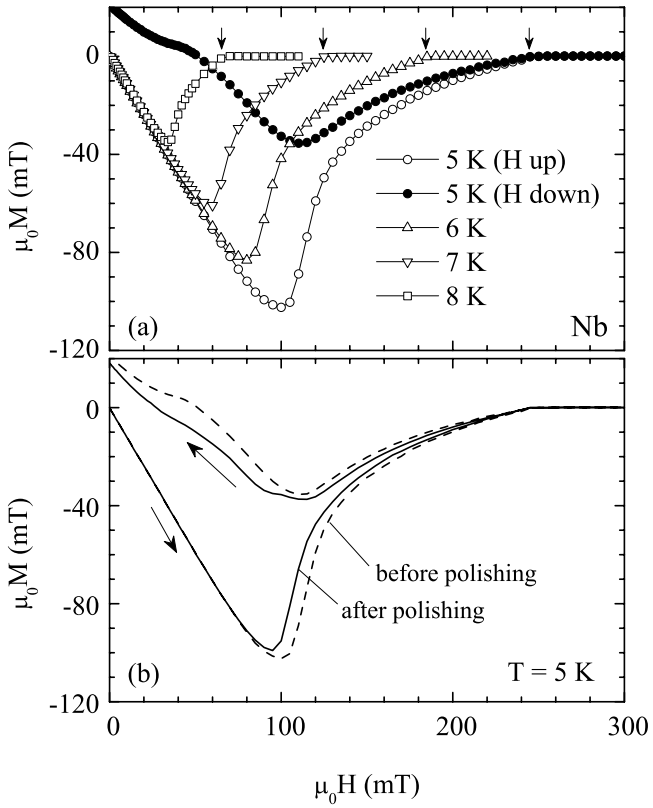

Figure 1. (a) Some examples of the magnetization versus magnetic field of the Nb single crystal, obtained at various constant temperatures below T_{C0}. The open symbols were obtained by increasing the external magnetic field, while the closed ones by decreasing it. The arrows indicate the upper critical magnetic field for each temperature. (b) $M(H)_T$ curves for $T = 5$ K before and after a chemical polishing of the crystal surfaces. After the surface treatment, the irreversibility is reduced to 50% its original value. This indicates that the pinning is mainly due to surface irregularities instead of inhomogeneities in the bulk.

$\sim$0.7 cm in height and $\sim$0.6 cm in diameter. The magnetic measurements were performed with a commercial SQUID magnetometer (Quantum Design, model MPMS). For magnetic fields below $\mu_0 \mathrm{H} = 1$ T, in our experiments, the resolution in magnetic moment is 10^{-11} A m^{-2}. This resolution, together with the relatively large size of the sample, allowed us to measure the FD well inside the short-wavelength region (where $\Delta M/H \lesssim 10^{-7}$ in SI units).

In order to check the samples' homogeneity and to obtain some superconducting parameters involved in the study of fluctuations (in particular the critical temperature and coherence length amplitude) we have performed measurements on the magnetization versus magnetic field for various temperatures below T_{C0}. Some examples of these measurements are shown in figures 1(a) and 2(a). The open symbols were obtained by increasing the external magnetic field, and the closed ones by decreasing it. The arrows indicate the critical magnetic field $H_C(T)$ in the case of Pb, and the upper critical magnetic field $H_{C2}(T)$ in the case of Nb. These last data are represented as a function of T in figure 2(b). As may be clearly seen, the temperature dependence is practically linear in the range studied. This allows us to linearly extrapolate to high and low temperatures. From the extrapolation to high temperatures we

determined the corresponding zero-field critical temperatures, T_{C0}. This leads to $T_{C0} = 7.20$ and 9.25 K for, respectively, the Pb and the Nb samples studied in this work. On the other hand, the extrapolation to $T = 0$ K leads to $\mu_0 H_{C2}(0) = 0.54$ T for Nb and $\mu_0 H_C(0) = 0.14$ T for Pb. In the case of type II Nb, by using the standard relation $\mu_0 H_{C2}(0) = \phi_0/2\pi\xi^2(0)$, we determined $\xi(0) = 250$ Å. These critical temperatures, magnetic fields and coherence lengths are in agreement with the values that may be found in the literature [6, 10]. In the case of the type I Pb, the coherence length amplitude was estimated through the expression $\phi_0/2\pi\xi^2(0) = \sqrt{2}\kappa H_C(0)$. By using the κ value of [10] ($\sim$0.3) we obtained $\xi(0) = 680$ Å.

Let us stress that the excellent structural and stoichiometric quality of the samples is compatible with the non-reversible behaviour of the magnetization observed in figures 1(a) and 2(a). In fact, as is now well established [11], in good quality (*soft*) samples the irreversibility is mainly due to *pinning* by the surface irregularities and not to inhomogeneities in the bulk. In order to check this we smoothed the original Nb crystal (which showed a rugosity characterized by an angle of $\sim 3°$) by immersing it for a few seconds in a solution of nitric and fluorhidric acids (in a proportion of 1:2). An example of the measured $M(H)$ behaviour in the Nb crystal after this surface treatment is presented in figure 1(b). As can be seen in this figure, the irreversibility was reduced by more than 50%, whereas the properties depending on the bulk quality, like the critical temperature or the coherence length amplitude, remained unchanged. Furthermore, we checked that the FD, which mainly depends on these bulk parameters, also remained unchanged. We have also checked in other samples (Pb–In alloys) that ΔM above T_{C0} does not vary within the experimental uncertainties after the electrolytic deposition on the sample surface of a film of Cu, which suppresses the surface superconductivity existing up to H_{C3} in the uncoated sample. In other words, these results indicate that the surface superconductivity between $H_{C2}(T)$ and $H_{C3}(T)$ does not affect the measured FD above $T_C(H)$. This last result confirms and extends to high ε and h, early conclusions of Gollub and co-workers [6].

3. Experimental results

Two examples, each one corresponding to the Pb and Nb samples, of the as-measured magnetic susceptibility versus temperature obtained with constant applied magnetic fields, $M(T)_H/H$, are shown in figure 3. These data were obtained with external magnetic fields of 5 mT for the Pb crystal and 40 mT for the Nb, which correspond to similar reduced magnetic fields, $h \equiv H/[\phi_0/2\pi\mu_0\xi^2(0)] \approx 0.07$. The lines in these figures are the normal-state or background contribution, $M_B(T)_H/H$, which were obtained by a linear fit to the magnetic susceptibility measured between $\sim 2.5T_{C0}$ and $\sim 4T_{C0}$, a temperature region where fluctuation effects are expected to be negligible. Let us remark that in the temperature range from $\sim 2T_{C0}$ up to the highest studied temperatures ($\sim 5T_{C0}$), the data do not present any appreciable deviation from the linear behaviour. Moreover the $M(T)_H/H$ slope is very small ($<10^{-9}$ K^{-1} for Nb and $<10^{-8}$ K^{-1} for Pb). These last results indicate, therefore, that the so-determined background magnetizations are very well defined, and that the corresponding excess diamagnetisms are not affected by the choice of the background fitting region, provided that the lower temperature limit of this background region is above $\sim 2.5T_{C0}$.

Some examples of the excess magnetization around T_{C0}, defined as $\Delta M(T)_H \equiv M(T)_H - M_B(T)_H$, normalized by their corresponding H amplitudes, are presented in figures 4(a) and (b). These curves already illustrate, at a qualitative level, some of the aspects that we are studying in this paper. Note first that these curves are strongly affected by the magnetic fields: even for the lowest fields used, which correspond to reduced fields of the order of $h = 10^{-3}$, the curves for different values of H do not agree with each other, at least at any temperature where the FD effects are perceptible. As for these low values of h, the conventional (or Prange) finite

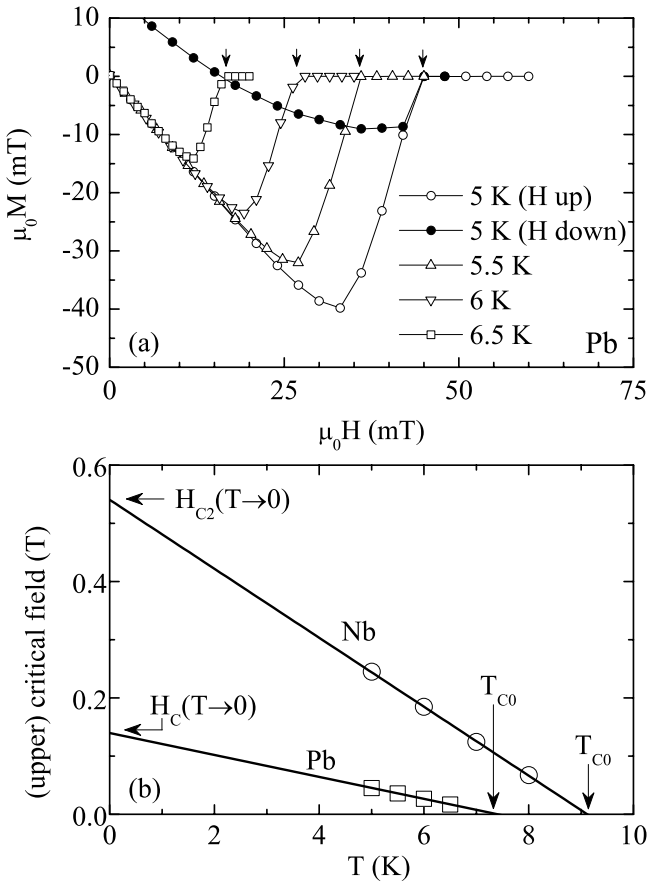

Figure 2. (a) Some examples of the magnetization versus magnetic field of the Pb single crystal, obtained at various constant temperatures below T_{C0}. The open symbols were obtained by increasing the external magnetic field, while the closed ones by decreasing it. The arrows indicate the upper critical magnetic field for each temperature. (b) Temperature dependence of the Nb upper critical field, H_{C2}, and Pb critical field, H_C. The corresponding $H_{C2}(T \to 0\,\mathrm{K})$ and $H_C(T \to 0\,\mathrm{K})$ values, as well as the critical temperatures, T_{C0}, were obtained through linear extrapolation.

field effects are expected to be negligible (see next section and also [1–6]). This result already suggests that the FD in these low-κ compounds is deeply affected by non-local electrodynamic effects that will manifest, even at these low-h values, by reducing the FD amplitude well below its value in the zero field limit. Such a behaviour is well illustrated by the results presented in figure 5, where $\Delta M/H$ is represented as a function of h. These data have been normalized to the theoretical value in the so-called zero-magnetic field (or Schmidt and Schmid) limit (this limit will be detailed in the next section). As can be seen in this figure, the results for both the Nb and the Pb samples are well below this theoretical limit, even for the lowest h. In addition, mainly in the case of the Nb sample where we have obtained FD data at very low h values, $\Delta M(h)_\varepsilon/H$ always decreases when h increases. Such an h dependence of the normalized FD also manifests in the Pb sample when $h \gtrsim 0.1$ (which corresponds to $h/\varepsilon \gtrsim 1.7$). Below this h value, we do not have enough data to make any conclusions, although our present results suggest a saturation of the finite field effects at very low h in the case of the Pb compound. For comparison, in this figure we have also represented the data we had previously obtained for a

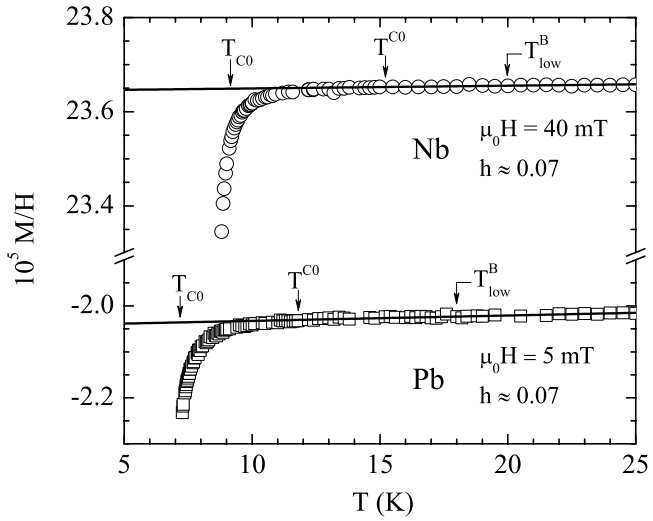

Figure 3. An example for each sample of the as-measured magnetic susceptibility against temperature at constant applied magnetic fields. The data shown were obtained with similar reduced magnetic fields, $h \approx 0.07$. The lines are the normal-state or background contributions. They were obtained by linear fit to the magnetic susceptibility measured between $\sim 2.5T_{C0}$ and $\sim 4T_{C0}$, a temperature region where fluctuation effects are expected to be negligible. T^B_{low} represents the lower limit of the background fitting region, and T^{C0} the temperature at which the fluctuations vanish at low magnetic fields ($h \lesssim 0.1$).

dirty Pb–18 at.% In (PbIn18%) alloy, with a much bigger Ginzburg–Landau parameter [5]. As can be seen in figure 5, this dirty alloy is much less affected by the non-local electrodynamic effects: not only is the corresponding $\Delta M(h)_\varepsilon/H$ independent of h when $h/\varepsilon < 1$, but also in this regime the corresponding amplitude agrees with the theoretical one for the zero-field limit. In spite of these important differences, we may also see in figure 5 that for the three compounds the excess diamagnetism becomes non-measurable for reduced fields near $h = 1$. We will argue in the next section that this FD suppression can be understood in terms of the limits imposed by the uncertainty principle to the shrinkage of the superconducting wavefunction when h increases [3].

The data of figures 4(a) and (b) also suggest that the FD amplitude vanishes in both compounds at a well defined temperature, T^{C0}, which is h independent up to $h \lesssim 0.2$: T^{C0} is of the order of 15 K for Nb and 12 K for Pb. This conclusion is clearly confirmed by the data of figures 6(a) and (b), where $-\Delta M/HT$ is represented as a function of ε in a double-logarithmic scale. In both compounds, the FD vanishes at a similar reduced temperature, which is of the order of $\varepsilon^{C0} \equiv \ln(T^{C0}/T_{C0}) \approx 0.5$. This value of ε^{C0} agrees, well within the experimental uncertainties, with the ε^{C0} values we have measured previously in other low-T_C and high-T_C compounds, with moderate or high κ values, much less affected by non-local electrodynamic effects [3–5]. This conclusion is illustrated in figure 7, where we compare different $\Delta M(\varepsilon)_h/HT$ curves for the Nb and the Pb samples studied here, with the data obtained before [5] in a dirty PbIn18% compound. To make the comparison between the results for the three different compounds easier, the data in this figure are divided by the corresponding theoretical FD values at $\varepsilon = 10^{-2}$ (see next section). The non-zero ΔM showed by some data points above $\varepsilon \approx 0.6$ in figures 6 and 7 may be attributed to experimental noise that becomes relevant at very low magnetization amplitudes. Despite the fact that the Pb–In

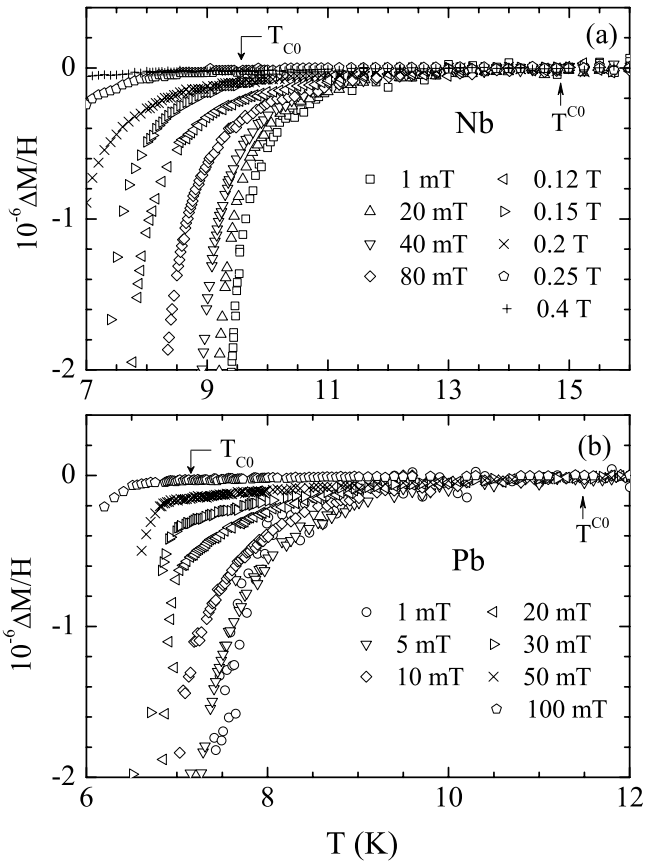

Figure 4. Some examples for (a) Nb and (b) Pb of the fluctuation-induced magnetization versus temperature curves normalized to their corresponding magnetic field amplitudes. The arrows indicate the corresponding zero-field critical temperatures, T_{C0}, and the temperatures, T^{C0}, at which the fluctuation effects at low fields ($h \lesssim 0.1$) vanish.

alloy is not appreciably affected by non-local electrodynamic effects, its corresponding FD also vanishes for $\varepsilon \gtrsim 0.5$. These results suggest, therefore, that even in the presence of non-local effects the high reduced temperature behaviour of the superconducting fluctuations in low-κ superconductors are still dominated by the limit imposed by the uncertainty principle to the shrinkage of the superconducting wavefunction when ε increases. This conclusion will be also examined at a quantitative level in the next section.

4. Comparison with the extended GGL approach

4.1. Theoretical background: extension of the GGL FD to the short wavelength regime

To analyse the experimental data summarized in the previous section, we will use the FD expressions calculated in [4] and [5] on the grounds of the mean-field GGL approach regularized through a so-called 'total energy' cutoff, which extends its applicability to the short-wavelength fluctuation regime. These previous calculations were centred on the high-ε region, up to ε^{C0}. The physical meaning of the total-energy cutoff was analysed in terms of the uncertainty

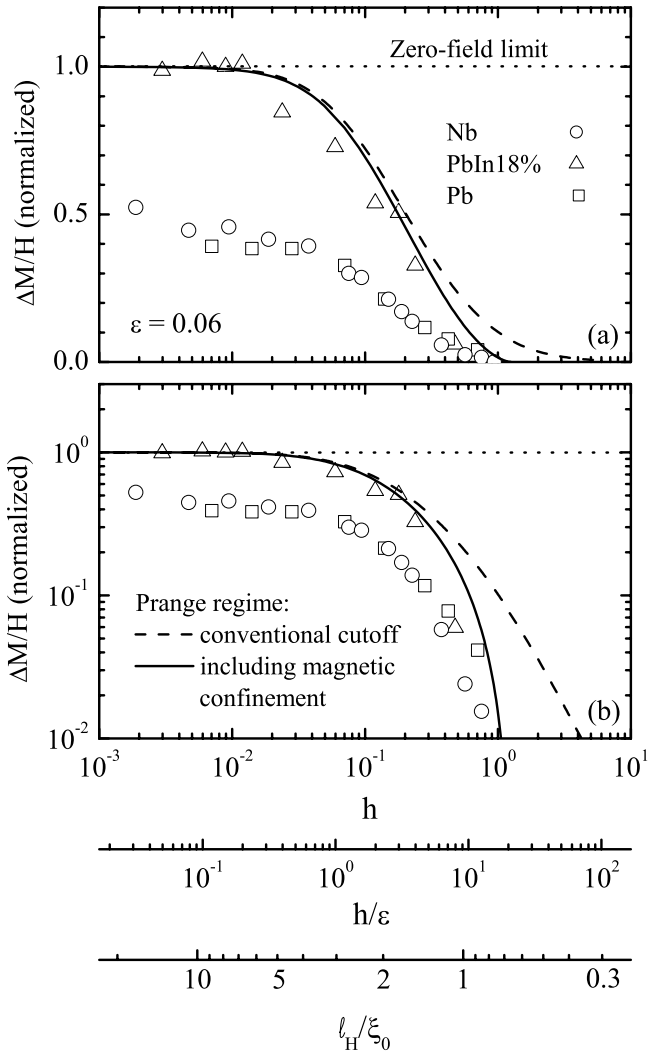

Figure 5. Magnetic field dependence of the fluctuation-induced magnetization (over H) at a constant reduced temperature for the Nb and Pb samples. These data are normalized to the theoretical GL value in the zero-field limit. The lines are the result of the GGL approach in the finite-field (or Prange) regime under different cutoff conditions. The important amplitude differences with the theoretical zero field limit are due to non-local electrodynamic effects. For comparison, also shown are some data from [5] corresponding to a higher-κ superconducting alloy (Pb–18 at.% In). These latter data extend up to $h \approx 0.6$. For this latter compound, the finite-field effects manifest for $h \gtrsim 2 \times 10^{-2}$ that, as it can be seen in the h/ε scale, corresponds well to $h/\varepsilon \gtrsim 0.1$. The Prange approach under a conventional cutoff is in excellent agreement with the experimental data up to $h \lesssim 0.3$ ($h/\varepsilon \lesssim 3$). These last results confirm, therefore, that the non-local effects are not appreciable in this dirty alloy, with a moderate value of κ. In the two clean superconductors, to explain the FD vanishing at $h \approx 1$ ($h/\varepsilon \approx 10$) one has to introduce a cutoff which takes into account the magnetic confinement energy. As is clearly seen in the third horizontal scale, for the two clean samples the FD vanishing occurs at a h amplitude which corresponds to $\ell_H \equiv \xi(0)h^{-1/2} \approx \xi_0$. The effects of magnetic confinement already manifest when $\ell_H \lesssim 2\xi_0$.

principle applied to the superconducting wavefunction in [3]: the existence of a well defined temperature, T^{C0}, above which all the superconducting fluctuations vanish, is directly related

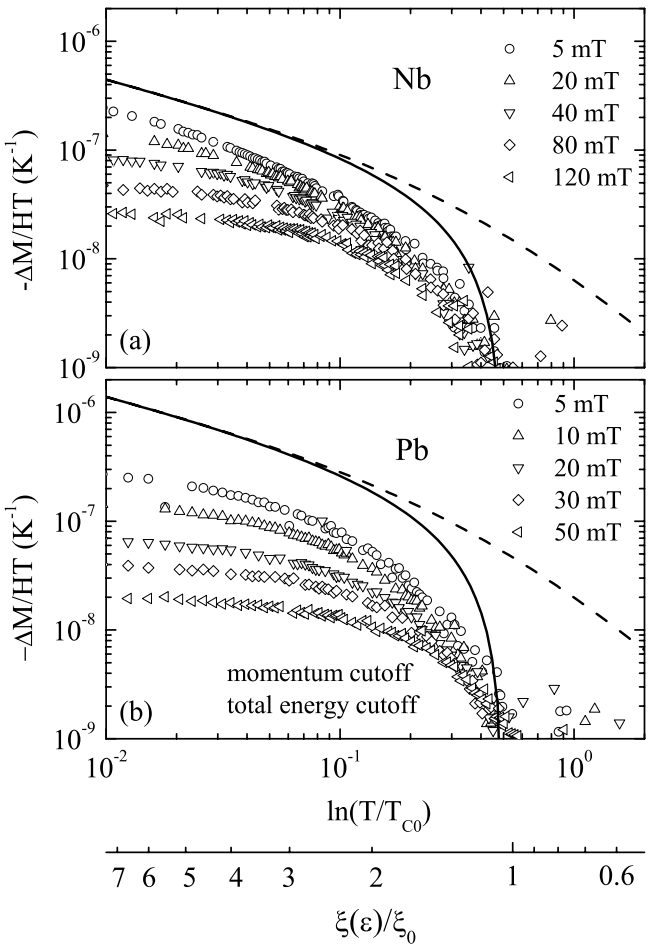

Figure 6. Reduced-temperature dependence of the fluctuation-induced magnetization (over HT) for various applied magnetic fields. The curves correspond to the zero-field limit under different cutoff conditions: the conventional momentum or kinetic energy cutoff and the so-called total energy cutoff, which includes the contribution associated with the shrinkage of the superconducting wavefunction at high ε. They were obtained by using the Nb and Pb coherence length amplitudes obtained in section 2, and with a cutoff constant of $c = 0.5$. As may be clearly seen, the zero-field limit amplitude is not reached even at the lowest magnetic field amplitudes, suggesting that non-local electrodynamic effects are quite important in these low-κ materials. However, for all field amplitudes the FD vanishes at the critical temperature $\varepsilon^{C0} \approx 0.5$ predicted for clean BCS superconductors when applying the uncertainty principle to the superconducting wavefunction. The data points above $\varepsilon \approx 0.6$ may be attributed to experimental noise. As illustrated in the lower scale, such a reduced temperature corresponds to $\xi(\varepsilon)/\xi_0$ of the order of 1.

to the limitations imposed by the uncertainty principle to the shrinkage of the superconducting wavefunction when the temperature increases above T_C. At low or moderate applied magnetic fields, when $h/\varepsilon \lesssim 1$, such a limitation associated with the uncertainty principle may be introduced through the superconducting coherence length in the zero-field limit, $\xi(\varepsilon)$, which even above T_{C0} cannot be smaller than ξ_0, the Pippard coherence length amplitude [3]. Well inside the finite field regime, when $h/\varepsilon \gg 1$, the characteristic length of the superconducting wavefunction when H varies will be, instead of $\xi(\varepsilon)$, of the order of the so-called magnetic

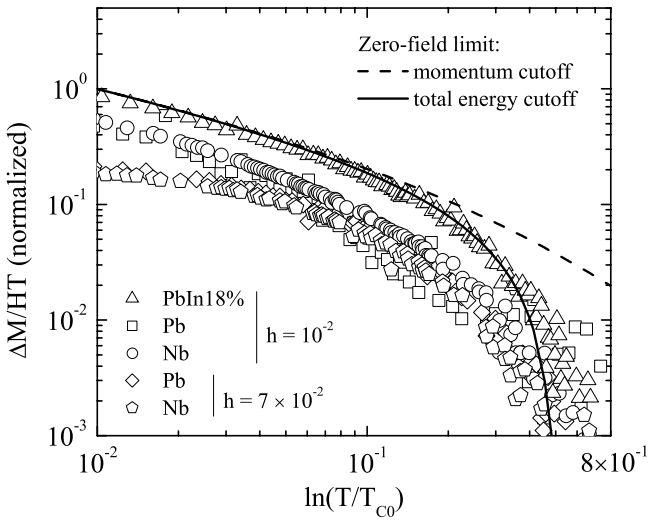

Figure 7. Reduced-temperature dependence of the fluctuation-induced magnetization (over HT) of Nb and Pb for two constant reduced magnetic fields. These data are normalized by the corresponding theoretical value in the zero-field limit at $\varepsilon = 10^{-2}$. The curves correspond to the zero-field theoretical approach under different cutoff conditions. As it may be clearly seen, these data almost scale, for each superconductor, for similar h values and they are also strongly reduced from the zero-field limit result. For comparison, some data from [5] corresponding to a higher-κ superconducting alloy (Pb–18 at.% In) obtained with $h = 2 \times 10^{-2}$ are also shown. In this last case, at all reduced temperatures the data are in excellent agreement with the zero-field limit approach. This last result confirms, therefore, the absence at all reduced temperatures of non-local electrodynamic effects in this dirty alloy. The data points above $\varepsilon \approx 0.6$ may be attributed to experimental noise.

length, $\ell_H \equiv \xi(0)h^{-1/2}$ [1, 2]. So, we will argue here that a natural extension of these ideas to the high-field regime is, when h varies, to impose the limitations associated with the uncertainty principle to the magnetic length. Therefore, it will be useful to first summarize in this subsection some of the results of such calculations for the case of bulk (3D) isotropic superconductors, which is the one well adapted to the compounds studied here. In this case, the total energy cutoff for zero applied magnetic field may be written as

$$k^2 + \xi^{-2}(\varepsilon) \leqslant \xi_0^{-2}, \tag{1}$$

where k is the wavevector of fluctuating modes. The left-hand side of equation (1) is the 'total energy' of a fluctuating mode in units of $\hbar^2/2m^*$, where $\hbar$ is the reduced Planck constant and m^* is the effective mass of the superconducting pairs. As explained in [3], this 'total energy' of each fluctuating mode may be seen as the sum of the Heisenberg localization energy associated with the shrinkage of the superconducting wavefunction when the temperature increases above T_C (the $\xi^{-2}(\varepsilon)$ term) and the conventional kinetic energy (the term proportional to k^2). The right-hand side in equation (1) may be seen as the Heisenberg localization energy associated to the maximum shrinkage, at $T = 0$ K, of the superconducting wavefunction. This term is, therefore, proportional to the inverse square of the Pippard coherence length amplitude, ξ_0.

Near T_{C0}, when $\xi(\varepsilon) \gg \xi_0$, the quantum localization contribution to the total energy of each fluctuating mode may be neglected, and equation (1) reduces then to the conventional momentum or kinetic-energy cutoff [1, 2]:

$$k^2 \leqslant c\xi^{-2}(0), \tag{2}$$

where instead of ξ_0 we have used $c^{-1/2}\xi(0)$, where c is a cutoff amplitude, temperature independent, close to 1. By also using $\xi_0 = c^{-1/2}\xi(0)$ in equation (1) and assuming the applicability at all reduced temperatures not too close to T_{C0} of the mean-field ε-dependence of the superconducting coherence length, $\xi(\varepsilon) = \xi(0)\varepsilon^{-1/2}$, one may see that the conventional kinetic-energy and the total-energy cutoff are related through the substitution of c by $c - \varepsilon$. Moreover, as stressed before, both cutoffs coincide near T_{C0}, when $\varepsilon \ll c$. The conventional momentum or kinetic-energy cutoff appears then as a particular case, the limit when $\xi(\varepsilon) \gg \xi_0$, of the total-energy cutoff. However, in spite of the simple relationship between both cutoff approaches, first proposed in [4], their deep conceptual differences also lead to striking differences in the high-ε behaviour of any quantity associated with the superconducting fluctuations above T_C, including the FD. These differences have been analysed in [3–5], but it could be useful to stress some of them here. Note first, that the maximum kinetic energy of the fluctuating Cooper pairs, $E^{max}_{kinetic}$, is temperature independent in the case of the conventional kinetic-energy or momentum cutoff:

$$E^{max}_{kinetic}(\text{momentum cutoff}) = \frac{\hbar^2 k^2_{max}}{2m^*} = \frac{\hbar^2}{2m^*\xi^2(0)}c. \tag{3}$$

In contrast, under a total-energy cutoff, the maximum kinetic energy of the Cooper pairs is temperature dependent. The corresponding $E^{max}_{kinetic}$ may be directly obtained from equation (3) by using $c - \varepsilon$ instead of c (or from equation (1) and using again $\xi_0 = c^{-1/2}\xi(0)$ and $\xi(\varepsilon) = \xi(0)\varepsilon^{-1/2}$) as:

$$E^{max}_{kinetic}(\text{total-energy cutoff}) = \frac{\hbar^2 k^2_{max}}{2m^*} = \frac{\hbar^2}{2m^*\xi^2(0)}(c - \varepsilon), \qquad \text{with } \varepsilon \leqslant c, \tag{4}$$

which is temperature dependent and becomes zero for $\varepsilon \geqslant c$. In other words, in contrast to the conventional momentum or kinetic-energy cutoff which only eliminates, independent of the temperature, the fluctuating modes with kinetic energy above $c\hbar^2/2m^*\xi^2(0)$, the total-energy cutoff eliminates *all* the fluctuation modes at reduced temperatures equal to c or above. By imposing a zero kinetic energy in equation (1), this reduced temperature, denoted ε^{C0}, is given by:

$$\xi(\varepsilon^{C0}) = \xi_0, \tag{5}$$

i.e., $\varepsilon^{C0} = (\xi(0)/\xi_0)^2 = c$. As first argued in [3], equation (5) (which leads directly to the existence of a well-defined reduced temperature above which all coherent Cooper pairs vanish) may be seen as just a consequence of the limitations of the uncertainty principle to the shrinkage of the superconducting wavefunction, which above T_{C0} also imposes the condition $\xi(\varepsilon) \geqslant \xi_0$. In other words, the collective behaviour of the Cooper pairs will be dominated at high reduced temperatures by the Heisenberg localization energy. If, in addition, we assume the applicability of the BCS relationship in the clean limit, $\xi(0) = 0.74\xi_0$, then $\varepsilon^{C0}_{BCSclean} = c_{BCSclean} \approx 0.5$ [3–5]. Indeed, this value of c will also apply to the conventional momentum cutoff approach, that appears as the limit when $\varepsilon \ll 1$ of the total-energy cutoff.

It will also be useful to remember here, that the conventional GGL approach, including the $\varepsilon^{-1/2}$ dependence of $\xi(\varepsilon)$, is formally valid only in the ε region $\varepsilon_{LG} \lesssim \varepsilon \ll 1$, where ε_{LG} is the so-called Levanyuk–Ginzburg reduced temperature [7]. Nevertheless, the conventional GGL approximation was extended by different authors well beyond the $\varepsilon \ll 1$ condition through the introduction of a momentum or kinetic energy cutoff. These attempts, unsuccessful for $\varepsilon \gtrsim 0.2$, were discussed in [4, 5]. The short wavelength effects on the FD were already addressed beyond the conventional momentum cutoff approach by different authors in the case of the low-T_C superconductors [8, 9, 12]. However, as already stressed in [3–5] and [13], these approaches do not take into account the limitations imposed by the uncertainty principle

to the superconducting wavefunction, whose effects are dominant at high ε. As a result, the approaches proposed in [8, 9, 12] do not predict a sharp vanishing of the fluctuation effects at any temperature at all (see also footnote 19 in [13]).

The FD in a bulk isotropic 3D superconductor in the finite field or Prange regime ($h/\varepsilon \gtrsim 1$) and neglecting the dynamic and non-local electrodynamic effects, has been calculated in [5] on the grounds of the GGL approach regularized through the total energy cutoff condition given by equation (1) as:

$$\Delta M(\varepsilon,h,c)_E = -\frac{k_B T}{\pi\phi_0\xi(0)}\sqrt{2h}\int_0^{\sqrt{(c-\varepsilon)/2h}} \mathrm{d}x\left[\frac{c-\varepsilon}{2h} - \left(\frac{c}{2h}+x^2\right)\psi\left(\frac{1}{2}+\frac{c}{2h}+x^2\right)\right.$$
$$+\ \ln\Gamma\left(\frac{1}{2}+\frac{c}{2h}+x^2\right) + \left(\frac{\varepsilon}{2h}+x^2\right)$$
$$\left.\times\ \psi\left(\frac{1}{2}+\frac{\varepsilon}{2h}+x^2\right) - \ln\Gamma\left(\frac{1}{2}+\frac{\varepsilon}{2h}+x^2\right)\right], \tag{6}$$

where Γ and ψ are, respectively, the gamma and digamma functions, ϕ_0 is the magnetic flux quantum and the dimensionless variable x is related to the parallel (to the applied field) momentum, $k_\parallel$, of the fluctuations through $x = \xi(0)k_\parallel/\sqrt{h}$. Note that when $\varepsilon \ll h$ and, simultaneously, $\varepsilon \ll c$, equation (6) reduces to:

$$\Delta M(h,c) = -\frac{k_B T}{\pi\phi_0\xi(0)}\sqrt{2h}\int_0^{\sqrt{c/2h}} \mathrm{d}x\left[\frac{c}{2h} - \left(\frac{c}{2h}+x^2\right)\psi\left(\frac{1}{2}+\frac{c}{2h}+x^2\right)\right.$$
$$\left.+\ \ln\Gamma\left(\frac{1}{2}+\frac{c}{2h}+x^2\right) + x^2\psi\left(\frac{1}{2}+x^2\right) - \ln\Gamma\left(\frac{1}{2}+x^2\right)\right]. \tag{7}$$

As already stressed in [5], the above expression for ΔM, which always applies at $T = T_{C0}$, may be used to easily relate the cutoff procedures we are summarizing here to the empirical scaling field, H_S, introduced by Gollub and co-workers to explain their pioneering FD results in LTSC [6]. In these works, H_S was defined as the magnetic field at which the scaled magnetization, $\Delta M\phi_0^{3/2}/k_B T(\mu_0 H)^{1/2}$, decreases to one half of its saturation value at $T = T_{C0}$ predicted by the Prange approach without a cutoff. Such a saturation value may be obtained by applying $h \ll c$ to equation (7), which leads to $\Delta M\phi_0^{3/2}/k_B T(\mu_0 H)^{1/2} \approx 0.324$. By using this last value we obtain $H_S \approx 0.5cH_{C2}(0)$. Moreover, from (7) one may easily justify the empirical proposal of Gollub and co-workers that the scaled magnetization, $\Delta M\phi^{3/2}/k_B T(\mu_0 H)^{1/2}$ is, at $T = T_{C0}$, a universal function of H/H_S: the behaviour of $\Delta M(h,c)$ predicted by equation (7) only depends at T_{C0} on c/h. It was also observed by Gollub and co-workers [6] and then confirmed by other authors [8, 9, 12], that when the dynamic and non-local electrodynamic effects are important, H_S becomes dependent on the specific characteristics of each material and much smaller than $H_{C2}(0)$. When described in terms of a cutoff parameter, these results mean that c will also manifest this material dependence, and it will be much smaller than 1. Such an entanglement of the non-local and short-wavelength effects will make any analysis at T_{C0} of these short-wavelength effects ambiguous.

In the zero-field (or Schmidt and Schmid) limit, i.e., for $h \ll \varepsilon$, equation (6) reduces to

$$\Delta M(\varepsilon,h,c)_E = -\frac{k_B T}{6\pi\phi_0\xi(0)}h\left(\frac{\arctan\sqrt{(c-\varepsilon)/\varepsilon}}{\sqrt{\varepsilon}} - \frac{\arctan\sqrt{(c-\varepsilon)/c}}{\sqrt{c}}\right). \tag{8}$$

As noted before, ΔM in the zero field limit, but under the conventional momentum or kinetic-energy cutoff, may be directly obtained from equation (8) by just changing c to $c+\varepsilon$ in the above equation. This leads to

$$\Delta M(\varepsilon,h,c)_M = -\frac{k_B T}{6\pi\phi_0\xi(0)}h\left(\frac{\arctan\sqrt{c/\varepsilon}}{\sqrt{\varepsilon}} - \frac{\arctan\sqrt{c/(\varepsilon+c)}}{\sqrt{\varepsilon+c}}\right). \tag{9}$$

Both expressions for ΔM in the zero-field limit reduces to the conventional (without cutoff) Schmidt and Schmid expression [14] when $\varepsilon \ll c$:

$$\Delta M(\varepsilon, h) = -\frac{k_B T}{12\phi_0 \xi(0)} \frac{h}{\sqrt{\varepsilon}}. \tag{10}$$

Although this paper is centred on the short wavelength fluctuations at high reduced temperatures ($\varepsilon \gtrsim 0.1$) and, simultaneously, low field amplitudes ($h \lesssim 0.1$), it will be useful to briefly present here a crude analysis of these short wavelength effects on the FD at high magnetic fields ($h \gtrsim 0.1$) and, simultaneously, low reduced temperatures ($\varepsilon \lesssim 0.1$). In this case the condition $h/\varepsilon \gg 1$ is quite well fulfilled and then, as we have already noted at the beginning of this subsection, the shrinkage of the superconducting wavefunction when h increases at constant ε may be parametrized through the magnetic length, ℓ_H, as

$$\xi(h)_\varepsilon = \frac{1}{b}\ell_H = \frac{1}{b}\xi(0)h^{-1/2}, \tag{11}$$

where b is a dimensionless constant (i.e., both temperature and magnetic field independent) expected to be of the order of 1. In this high-field regime the limitations imposed by the indetermination principle to the shrinkage of the superconducting wavefunction may be expressed as

$$\xi^{-2}(h)_\varepsilon < \xi_0^{-2}. \tag{12}$$

In turn, this condition limits the energy of the Cooper pairs created by thermal fluctuations through (in units of $\hbar^2/2m^*$)

$$E_{kinetic} + \xi^{-2}(h) \leqslant \xi_0^{-2}, \tag{13}$$

where we have already assumed $\varepsilon \ll h$ and, therefore, the term in $\xi^{-2}(\varepsilon)$ may be neglected. The term $\xi^{-2}(h)$ on the left-side of equation (13) may be seen as the Heisenberg localization energy associated with the shrinkage of the superconducting wavefunction when h increases. By taking into account $\xi_0 = c^{-1/2}\xi(0)$ and equation (11), (13) may be written as

$$E_{kinetic} \leqslant \xi^{-2}(0)(c - b^2 h). \tag{14}$$

Therefore, the comparison of equation (14) with (1) and (2) suggests that one may crudely take into account the limits imposed by the uncertainty principle to the magnetic confinement of the superconducting fluctuations by just changing c to $c - b^2 h$ in the phenomenological GGL expressions under a momentum or a total energy (equation (6)) cutoff. In other words, for 3D isotropic superconductors the FD at high reduced fields may be *crudely* approximated by just changing c to $c - b^2 h$ in equation (6). A more quantitative calculation of the FD taking into account the limitations imposed by the uncertainty principle to the magnetic confinement should start from the Ginzburg–Landau fluctuation free energy expression instead of directly from equation (6). However, this procedure is substantially complicated for the relevant range of high magnetic fields by the discreteness of the Landau-level spectrum of the superconducting fluctuations. A way to circumvent this difficulty could be to use a penalization function procedure similar to the one proposed by Patton and co-workers in [12]. Work is presently in progress to elaborate such calculations.

4.2. Comparison with the experimental data

The solid curves in figures 6(a) and (b) correspond to the FD calculated on the grounds of the GGL approach in the zero-field (or Schmidt and Schmid) limit and under a total-energy cutoff (equation (8)). At least for the data points measured under the lowest field amplitudes ($h = 6 \times 10^{-3}$ for Pb and 2×10^{-3} for Nb), such a zero-field approximation will be, in

principle, well adapted to the measurements shown in these figures, even at the lowest reduced temperatures. These solid curves were calculated by using in equation (8) the coherence length values obtained in section 2 from magnetization measurements below T_{C0}, and with the cutoff constant $c = 0.5$, the value estimated in the precedent subsection for clean BCS superconductors. One may see in these figures that for $\varepsilon \lesssim 0.1$ the theoretical FD amplitude strongly disagrees, by at least a factor of two, with the experimental one, even for those data measured under the lowest field amplitudes. As these last data are well in the zero field limit (i.e., $h/\varepsilon \ll 1$), these results provide a further confirmation that the FD in these two clean and low-κ superconductors are strongly affected by non-local electrodynamic effects. However, the central aspect shown by this comparison is that such a disagreement is strongly mitigated at high reduced temperatures, when $\varepsilon \gtrsim 0.3$. Moreover, this theoretical FD under the total-energy cutoff accounts at a quantitative level for the vanishing of the measured FD at $\varepsilon \approx 0.5$. In other words, the comparison between the theory and the experiments presented in figures 6(a) and (b) strongly suggests that even in presence of important non-local effects, at high reduced temperatures the FD is still dominated by the Heisenberg localization energy, which imposes a limit to the shrinkage of the superconducting wavefunction. To illustrate when such a contribution becomes important, in figure 6 we have included $\xi(\varepsilon)/\xi_0$ as a second horizontal scale. To estimate $\xi(\varepsilon)/\xi_0$ we have used the reduced temperature dependence of $\xi(\varepsilon)$ predicted by the mean-field approaches, $\xi(\varepsilon) = \xi(0)\varepsilon^{-1/2}$, and the BCS relationship between $\xi(0)$ and ξ_0 in the clean limit, $\xi(0) = 0.74\xi_0$. We see that the FD is appreciably affected by the quantum localization when $\xi(\varepsilon)$ becomes of the order of ξ_0 (for $\xi_0 \lesssim \xi(\varepsilon) \lesssim 2\xi_0$).

In figures 6(a) and (b) we also compare the experimental FD curves with the theoretical results also in the zero field limit but under the conventional momentum or kinetic-energy cutoff: the dashed curves in these figures correspond to equation (8) with the same $\xi(0)$ and c values as before. Whereas at low reduced temperatures, for $\varepsilon \lesssim 0.1$, both theoretical approaches coincide, one may see that the differences become very important at high reduced temperatures, for $\varepsilon \gtrsim 0.1$. In particular, in contrast to the experimental results, the theoretical FD under the conventional momentum cutoff does not vanish at any reduced temperature. To further analyse the FD data obtained at low magnetic fields ($h < 0.1$), in figure 7 we compare the FD observed in Nb and Pb with the one corresponding to a dirty Pb–18 at.% In (Pb–In18%) alloy and with the theoretical FD calculated on the grounds of the zero-field GGL approach under both cutoff conditions. These different data were divided by the corresponding theoretical zero-field limit amplitudes at $\varepsilon = 2 \times 10^{-2}$. These theoretical amplitudes were calculated by using equation (8), with $c = 0.5$. As may be clearly seen in this figure, the data for the Pb–In dirty alloy (which has a higher κ-value than the Nb and Pb samples and much less important non-local effects) are in excellent agreement with the predictions of the total-energy cutoff approach, not only in what concerns to the FD vanishing at $\varepsilon \approx 0.5$, but also in the amplitude in the whole accessible reduced temperature range.

A first analysis of our FD results in the finite field regime is summarized in figures 5(a) and (b). Here we present the FD h-dependence of the Nb, Pb and, for comparison, PbIn18% samples, normalized to the theoretical low-field value under a cutoff ($c = 0.5$). As commented above, only the data corresponding to the dirty Pb–In alloy reach the zero-field limit FD amplitude. These last results, which were taken from [5], show that non-local effects are unobservable in this dirty and relatively high-κ compound. As may be seen in the second horizontal scale (where it is shown as h/ε), the finite field effects appear for $h/\varepsilon \gtrsim 2 \times 10^{-1}$. In this region the FD amplitude decreases considerably with respect to the low-field limiting value. The dashed curve is the GGL finite-field approach under a conventional cutoff (equation (14)), evaluated with $c = 0.5$. This approach accounts for the experimental data of PbIn18% up to $h/\varepsilon \approx 6$. The same can be said for the h dependence of the FD corresponding to the Nb and Pb

samples. For the two clean superconductors the experimental FD vanishes at $h \approx 1$ while the conventional cutoff approach predicts a non-zero FD at all h values. This may be seen better in the log–log representation of figure 5(b). As commented above, the FD vanishing at $h \approx 1$ may be associated to the limits imposed by the uncertainty principle to the shrinkage of the superconducting wavefunction induced by the application of a magnetic field. The solid curve in figures 5(a) and (b) is the best fit of equation (6), with $c - b^2 h$ instead of c, to the FD data of the PbIn18% alloy up to $h = 0.6$. In doing that fit we imposed $c = 0.5$ and left b as the only free parameter. As may be clearly seen, this approach is in excellent agreement with the FD data of the PbIn18% alloy, and also with the behaviour of the two clean superconductors when $h \to 1$. The third horizontal scale in figure 5 indicates the magnetic length ℓ_H relative to the coherence length amplitude at $T = 0$ K. As is clearly seen, for the two clean samples the FD vanishes just at the reduced magnetic field at which $\ell_H \approx \xi_0$. This seems to confirm the idea that the superconducting fluctuations cannot be confined to lengths smaller than the coherence length amplitude at $T = 0$ K, independent of the fact that the confinement is induced by high reduced temperatures or by high reduced magnetic fields. However, in these clean samples the FD is also strongly reduced by non-local electrodynamic effects when h increases [8, 9] and, therefore, measurements at high reduced fields in dirty alloys, much less affected by non-local effects [1, 2, 5, 9], will be of crucial importance to determine quantitatively the value of the reduced field at which the superconducting fluctuations vanish (which, once the non-local effects are suppressed, may be somewhat bigger than $h = 1$) and also to establish the universality and the physical origin of the pair breaking mechanism when $h \to 1$.

5. Conclusions

We have presented in this paper detailed measurements of the FD in two clean low-T_C superconductors: a type I superconductor (Pb) and a low-κ type II superconductor (Nb). These measurements cover, to the best of our knowledge for the first time, both the high reduced temperature regime and the high reduced magnetic field regime in clean and low-κ superconductors. These results were then analysed in terms of the GGL approaches, extended to the short wavelength regime by introducing a so-called total-energy cutoff, which takes into account the quantum localization energy contribution associated with the shrinkage of the superconducting wavefunction. Our results strongly suggest that despite the fact that in these superconductors the FD is deeply affected by non-local electrodynamic effects, the short wavelength fluctuations are still dominated by the uncertainty principle which imposes a limit to the shrinkage, when ε or h increases, of the superconducting wavefunction. When compared with our previous results in dirty low-T_C and in clean high-T_C superconductors, these results suggest the universality of these quantum limits to the superconducting fluctuations when $\varepsilon \to c \approx 0.5$. Measurements at high fields in dirty low-T_C superconductors, less affected by non-local effects, are now in progress to determine quantitatively the value of the reduced field at which the superconducting fluctuations vanish and to try to establish the physical origin and the universality of the non-conventional FD behaviour observed in the present work in clean low-T_C superconductors when $h \to 1$.

Acknowledgments

This work has been supported by Unión Fenosa under grant no 0666/02, by the CICYT, Spain under grants MAT2001-3272 and MAT2001-3053, and by the Xunta de Galicia under grant PGIDIT01PXI20609PR.

References

[1] Skocpol W J and Tinkham M 1975 *Rep. Prog. Phys.* **38** 1049

[2] Tinkham M 1996 *Introduction to Superconductivity* (New York: McGraw-Hill) ch 8 and references therein

[3] Vidal F, Carballeira C, Currás S R, Mosqueira J, Ramallo M V, Veira J A and Viña J 2002 *Europhys. Lett.* **59** 754 (*Preprint* cond-mat/0112486) and references therein
Following Pippard's pioneering proposal below T_C,
Pippard A B 1953 *Proc. R. Soc.* A **216** 547
see also
De Gennes P G 1966 *Superconductivity of Metals and Alloys* (New York: Benjamin) sections 1–4
in our paper the uncertainty principle was applied to the superconducting wavefunction above T_C by using the original Heisenberg version, i.e., in terms of the momentum of each fluctuating mode and the characteristic length of the superconducting wavefunction. However, qualitatively one may reach the same conclusions *above* T_C by using the Bohr version of the uncertainty principle, in terms of the lifetime of the fluctuating Cooper pairs and the driving thermal agitation energy, $k_B T$. Let us also note here that it is now well established that the superconductivity may still remain when the size of the sample is reduced well below the ξ_0 of the bulk material see, e.g.,
von Delft J and Ralph D C 2001 *Phys. Rep.* **345** 61 and references therein
indeed, this is not in contradiction with equations (1) and (12) because in such small superconductors the coherence length will loss its conventional meaning.

[4] Mosqueira J, Carballeira C, Ramallo M V, Torrón C, Veira J A and Vidal F 2001 *Europhys. Lett.* **53** 632
Carballeira C, Currás S R, Viña J, Veira J A, Ramallo M V and Vidal F 2001 *Phys. Rev.* B **63** 144515
Viña J, Campá J A, Carballeira C, Currás S R, Maignan A, Ramallo M V, Rasines I, Veira J A, Wagner P and Vidal F 2002 *Phys. Rev.* B **65** 212509
Carballeira C, Ramallo M V and Vidal F 2001 *J. Phys.: Condens. Matter* **13** 2573
Carballeira C, Mosqueira J, Revcoleschi A and Vidal F 2003 *Physica* C **384** 185

[5] Mosqueira J, Carballeira C and Vidal F 2001 *Phys. Rev. Lett.* **87** 167009
Carballeira C, Mosqueira J, Ramallo M V, Veira J A and Vidal F 2001 *J. Phys.: Condens. Matter* **13** 9271
Mosqueira J, Ramallo M V, Currás S R, Torrón C and Vidal F 2002 *Phys. Rev.* B **65** 174522

[6] Gollub J P, Beasley M R, Newbower R S and Tinkham M 1970 *Phys. Rev. Lett.* **25** 1646
Gollub J P, Beasley M R, Callarotti R and Tinkham M 1973 *Phys. Rev.* B **7** 3039

[7] See, e.g.,
Vidal F and Ramallo M V 1998 *The Gap Symmetry and Fluctuations in High T_c Superconductors* ed J Bok, G Deutscher, D Pavuna and S A Wolf (London: Plenum) p 477

[8] Lee P A and Payne M G 1971 *Phys. Rev. Lett.* **26** 1537

[9] Kurkijärvi J, Ambegaokar V and Eilenberger G 1972 *Phys. Rev.* B **5** 868

[10] Poole Ch Jr 2000 *Handbook of Superconductivity* (San Diego, CA: Academic)

[11] See, e.g.,
Lazard G, Mathieu P, Plaçais B, Mosqueira J, Simon Y, Guilpin C and Vacquier G 2002 *Phys. Rev.* B **65** 064518 and references therein

[12] Patton B R, Ambegaokar V and Wilkins J W 1969 *Solid State Commun.* **7** 1287
Patton B R and Wilkins J W 1972 *Phys. Rev.* B **6** 4349

[13] Mosqueira J, Ramallo M V, Currás S R, Torrón C and Vidal F 2002 *Phys. Rev.* B **65** 174522

[14] Schmidt H 1968 *Z. Phys.* **43** 336
Schmid A 1969 *Phys. Rev.* **180** 527